

Gradient boosting for extreme quantile regression

Jasper Velthoen ^{*} Clément Dombry [†] Juan-Juan Cai [‡]
 Sebastian Engelke [§]

December 23, 2024

Abstract

Extreme quantile regression provides estimates of conditional quantiles outside the range of the data. Classical methods such as quantile random forests perform poorly in such cases since data in the tail region are too scarce. Extreme value theory motivates to approximate the conditional distribution above a high threshold by a generalized Pareto distribution with covariate dependent parameters. This model allows for extrapolation beyond the range of observed values and estimation of conditional extreme quantiles. We propose a gradient boosting procedure to estimate a conditional generalized Pareto distribution by minimizing its deviance. Cross-validation is used for the choice of tuning parameters such as the number of trees and the tree depths. We discuss diagnostic plots such as variable importance and partial dependence plots, which help to interpret the fitted models. In simulation studies we show that our gradient boosting procedure outperforms classical methods from quantile regression and extreme value theory, especially for high-dimensional predictor spaces and complex parameter response surfaces. An application to statistical post-processing of weather forecasts with precipitation data in the Netherlands is proposed.

Keywords: extreme quantile regression; gradient boosting; generalized Pareto distribution; extreme value theory; tree-based methods.

^{*}Department of Applied Mathematics, Delft University of Technology, Mekelweg 4 2628 CD Delft. E-mail: j.j.velthoen@tudelft.nl

[†]Université Bourgogne Franche-Comté, Laboratoire de Mathématiques de Besançon, CNRS UMR 6623, F-25000 Besançon, France. E-mail: clement.dombry@univ-fcomte.fr

[‡]Department of Econometrics and Data Science, Vrije Universiteit Amsterdam, De Boelelaan 1105, 1081HV, Amsterdam, the Netherlands. E-mail: j.cai@vu.nl

[§]Research Center for Statistics, University of Geneva, Boulevard du Pont d'Arve 40, 1205 Geneva, Switzerland. E-mail: sebastian.engelke@unige.ch

1 Introduction

In a regression setup the distribution of a quantitative response Y depends on a set of covariates (or predictors) $\mathbf{X} \in \mathbb{R}^d$. These predictors are typically easily available and can be used to predict conditional properties of the response variable Y . Machine learning offers a continuously growing set of tools to perform prediction tasks based on a sample $(\mathbf{X}_1, Y_1), \dots, (\mathbf{X}_n, Y_n)$ of independent copies of a random vector (\mathbf{X}, Y) . The main objective is usually to predict the conditional mean $\mathbb{E}(Y \mid \mathbf{X} = \mathbf{x})$, which corresponds to minimizing the squared error prediction loss. While the mean summarizes the behavior of Y in the center of its distribution, applications in the field of risk assessment require knowledge of the distributional tail. For a probability level $\tau \in (0, 1)$, an important quantity is the conditional quantile

$$Q_{\mathbf{x}}(\tau) = F_Y^{-1}(\tau \mid \mathbf{X} = \mathbf{x}), \quad (1)$$

where $F_Y^{-1}(\cdot \mid \mathbf{X} = \mathbf{x})$ is the generalized inverse of the conditional distribution function of Y . There has been extensive research in statistics and machine learning to adapt mean prediction methods to other loss functions than squared error. For instance, quantile regression relies on minimizing the conditional quantile loss, which is based on the quantile check function ([Koenker and Bassett Jr, 1978](#)). This has been extended to more flexible regression functions such as the quantile regression forest ([Meinshausen, 2006](#)) and the gradient forest ([Athey et al., 2019](#)), which both build on the original random forest ([Breiman, 2001](#)). Another popular tree-based method in machine learning is gradient boosting by [Friedman \(2001\)](#). This versatile method aims at optimizing an objective function with a recursive procedure akin to gradient descent.

Let n denote the sample size and the quantile level $\tau = \tau_n$. The existing quantile regres-

sion methodology works well in the case of a fixed quantile level, or in the case of a quantile that is only moderately high, that is, $\tau_n \rightarrow 1$ and $n(1 - \tau_n) \rightarrow \infty$ as $n \rightarrow \infty$, meaning that there are sufficient observations above the τ_n level. For more extreme quantiles with $n(1 - \tau_n) \rightarrow 0$, the quantile loss function is no longer useful because observations become scarce at that level and extrapolation beyond the range of observed values is needed. Extreme value theory provides the statistical tools for a sensible extrapolation into the tail of the variable of interest Y . For a large threshold u close to the upper endpoint of the distribution of Y , the distribution of the threshold exceedance $Y - u \mid Y > u$ can be approximated by the generalized Pareto distribution (GPD)

$$H_{\gamma,\sigma}(y) = 1 - (1 + \gamma y/\sigma)_+^{-1/\gamma}, \quad y \geq 0, \quad (2)$$

where $a_+ = \max(0, a)$, and $\gamma \in \mathbb{R}$ and $\sigma > 0$ are the shape and scale parameters, respectively.

There are three main streams in the literature focusing on the estimation of covariate-dependent extreme quantiles. First, [Chernozhukov \(2005\)](#) and [Wang et al. \(2012\)](#) assume a linear form for the conditional quantile function in [\(1\)](#) and derive estimators and asymptotic properties for extreme quantiles. The second stream uses the GPD to model threshold exceedances with parameters σ and γ in [\(2\)](#) depending on the covariates via parametric or semi-parametric structures such as linear models ([Davison and Smith, 1990](#); [Wang and Tsai, 2009](#)) and generalized additive models ([Chavez-Demoulin and Davison, 2005](#); [Youngman, 2019](#)). A third direction is to first estimate the conditional quantiles at moderately high levels by local smoothing methods and then to extrapolate to the extreme level (e.g., [Daouia et al., 2013](#); [Gardes and Stupfler, 2019](#); [Velthoen et al., 2019](#)). While linear or additive models are restricted in their modelling flexibility, local smoothing methods on the other hand are known to be sensitive to the curse of dimensionality and work well only

for a low-dimensional predictor space. To account for these issues for modern applications with complex data, tree-based methods are attractive due to their modelling flexibility and robustness in higher dimensions. A first attempt to use tree-based models in extreme value theory is the generalized Pareto regression tree by [Farkas et al. \(2019\)](#), but the model reduces to a single tree and suffers from limited performance.

Our goal is to build a bridge between the predictive power of tree-based ensemble methods from machine learning and the theory of extrapolation from extreme value theory. We propose a two-step tree-based procedure that is relevant for risk assessment with many covariates and with complex non-linear effects. First, the gradient forest of [Athey et al. \(2019\)](#) is used to estimate intermediate conditional quantiles of order $\tau_0 > 0$, playing the role of a high threshold. Second, the exceedances above the threshold are modeled by a GPD distribution in [\(2\)](#) with covariate-dependent parameters $\gamma(\mathbf{x})$ and $\sigma(\mathbf{x})$. To estimate $\gamma(\mathbf{x})$ and $\sigma(\mathbf{x})$ we propose a gradient boosting algorithm to optimize the deviance (negative log-likelihood) of the GPD model conditional on the predictor value $\mathbf{X} = \mathbf{x}$. In each boosting iteration, these parameters are updated based on an approximation of the deviance gradient by regression trees. The boosting algorithm has several tuning parameters, the most important ones being the tree number and tree depth. We show how they can be chosen effectively using cross-validation. The resulting model includes many trees and is flexible enough to account for a complex non-linear response surface. Diagnostic tools are available such as variable importance score and partial dependence plots. In two numerical experiments we illustrate that, for the task of extremal quantile estimation, our methodology outperforms quantile regression approaches that do not use tail extrapolation ([Meinshausen, 2006](#); [Athey et al., 2019](#)) and methods from extreme value theory that assume simple forms for $\gamma(\mathbf{x})$ and $\sigma(\mathbf{x})$ such as generalized additive models ([Youngman,](#)

2019).

The paper is organized as follows. Section 2 introduces background on extreme quantile estimation and quantile regression forests. Our gradient boosting based method is developed in Section 3 with two main algorithms. Practical questions such as parameter tuning and model interpretation are discussed in Section 4, while Section 5 is devoted to assessing the performance of our method in two simulation studies. An application to statistical post-processing of weather forecasts with precipitation data in the Netherlands is given in Section 6.

The gradient boosting method is implemented in an R package and can be downloaded from GitHub at <https://github.com/JVelthoen/gbex/>

2 Background

2.1 Extreme quantile estimation

Extreme value theory provides the asymptotic results for extrapolating beyond the range of the data and statistical methodology has been developed to accurately estimate high quantiles. Most of these tools however do only apply in the case where Y_1, \dots, Y_n are independent copies of Y and do not depend on covariates.

In this case, the Pickands–de Haan–Balkema theorem (Balkema and de Haan, 1974; Pickands III, 1975) states that under mild regularity conditions on the tail of the distribution of Y , the rescaled distribution of exceedances over a high threshold converges to the generalized Pareto distribution. More precisely, if y^* denotes the upper endpoint of the

distribution of Y then there exist a normalizing function $\sigma(u) > 0$ such that

$$\lim_{u \uparrow y^*} \mathbb{P} \left(\frac{Y - u}{\sigma(u)} > y \mid Y > u \right) = 1 - H_{\gamma,1}(y), \quad y \geq 0, \quad (3)$$

where H is defined in (2), with the convention $H_{0,\sigma}(y) = 1 - \exp(-y/\sigma)$, $y \geq 0$. The shape parameter $\gamma \in \mathbb{R}$ indicates the heaviness of the upper tail of Y , where $\gamma < 0$, $\gamma = 0$ and $\gamma > 0$ correspond to distributions respectively with finite upper endpoint (e.g., uniform), light tails (e.g., Gaussian, exponential) and power tails (e.g., Student's t).

Moreover, the GPD is the only non-degenerate distribution that can arise as the limit of threshold exceedances as in (3), and therefore it is an asymptotically motivated model for tail extrapolation and high quantile estimation. By the limit relation in (3), for a large threshold u , the conditional distribution of $Y - u$ given $Y > u$ can be approximated by $H_{\gamma,\sigma}$ with $\sigma = \sigma(u)$. The threshold u can be chosen as the quantile $Q(\tau_0)$ of Y for some moderately high probability level $\tau_0 \in (0, 1)$. Inverting the distribution function in (2) provides an approximation of the quantile for probability level $\tau > \tau_0$ by

$$Q(\tau) \approx Q(\tau_0) + \sigma \frac{\left(\frac{1-\tau}{1-\tau_0} \right)^{-\gamma} - 1}{\gamma}. \quad (4)$$

2.2 Quantile regression forests

Quantile regression studies the problem of estimating the conditional quantile $Q_{\mathbf{x}}(\tau)$ defined in (1), based on $(\mathbf{X}_1, Y_1), \dots, (\mathbf{X}_n, Y_n)$ a sequence of independent copies of a random vector (\mathbf{X}, Y) with $\mathbf{X} \in \mathbb{R}^d$ and $Y \in \mathbb{R}$. Most approaches for quantile estimation rely on the property

$$Q_{\mathbf{x}}(\tau) = \underset{q}{\operatorname{argmin}} \mathbb{E} [\rho_{\tau}(Y - q) \mid \mathbf{X} = \mathbf{x}], \quad (5)$$

where $\rho_\tau(u) = (\tau - \mathbb{I}\{u < 0\})u$ is the quantile check function as introduced in [Koenker and Bassett Jr \(1978\)](#). Standard linear quantile regression assumes a linear form for q and the regression coefficients are obtained by solving an optimization problem corresponding to the empirical counterpart of (5). Without a parametric assumption on q , an estimator can be constructed pointwise by defining

$$\hat{Q}_{\mathbf{x}}(\tau) = \underset{q}{\operatorname{argmin}} \sum_{i=1}^n w_i(\mathbf{x}) \rho_\tau(Y_i - q). \quad (6)$$

where w_1, \dots, w_n is a sequence of localizing weight functions. For quantile regression there exists a rich literature with both parametric and non-parametric approaches to estimate conditional quantiles. For more details, we refer to the monograph [Koenker \(2005\)](#).

In this section we focus on quantile regression using random forests. The reason for this is three-fold: first it requires no parametric assumptions on the quantile functions; secondly it exhibits good performance for high dimensional predictor spaces; finally it requires minimal tuning for good results. Random forest as proposed by [Breiman \(2001\)](#) consists of B trees that are fitted to different bootstrap samples of the data. A tree is built by recursive binary splitting resulting in a finite partition of the predictor space into rectangular sub-spaces called leaves. We denote by $L_b(\mathbf{x}) \subset \mathbb{R}^d$ the leaf in the b th tree that contains \mathbf{x} . Then the b th tree assigns to each observation in $L_b(\mathbf{x})$ the following weight

$$w_{i,b}(\mathbf{x}) = \frac{\mathbb{I}\{\mathbf{X}_i \in L_b(\mathbf{x})\}}{\sum_{k=1}^n \mathbb{I}\{\mathbf{X}_k \in L_b(\mathbf{x})\}}. \quad (7)$$

Averaging over the B trees, we obtain the localizing weight functions

$$w_i(\mathbf{x}) = \frac{1}{B} \sum_{b=1}^B w_{i,b}(\mathbf{x}). \quad (8)$$

[Meinshausen \(2006\)](#) suggests to estimate the conditional quantile (6) using the random forest weights (8). The drawback of this method is that the criterion used in recursive binary

splitting to build the trees of the random forest aims at minimizing the squared error loss. Hence the localizing weight functions are designed for the prediction of the conditional mean. [Wager and Athey \(2018\)](#) therefore propose to define a generalized random forest by splitting with respect to different criteria designed for specific tasks. In the case of quantile regression, the criterion is related to the quantile loss function. The weights $w_i(\mathbf{x})$ are then defined in a similar way as above, but they result in more accurate estimation of the conditional quantiles. A detailed description of the construction of generalized random forests for quantile regression is given in [Appendix B](#).

3 GPD modeling with gradient boosting

3.1 Setup

We consider here the setting where the response $Y_i \in \mathbb{R}$ depends on covariates $\mathbf{X}_i \in \mathbb{R}^d$ and our goal is to develop an estimator for the conditional quantile $Q_{\mathbf{x}}(\tau_n)$ defined by [\(1\)](#), where the probability level τ_n satisfies $\tau_n \rightarrow 1$ and $n(1 - \tau_n) \rightarrow 0$ as $n \rightarrow \infty$. Such a quantile is extreme in the sense that the expected number of observations that exceed $Q_{\mathbf{x}}(\tau_n)$ converges to 0 as $n \rightarrow \infty$. Therefore empirical estimation is not feasible and extrapolation beyond observations is needed. Recall that $(\mathbf{X}_1, Y_1), \dots, (\mathbf{X}_n, Y_n)$ denote independent copies of the random vector (\mathbf{X}, Y) with $\mathbf{X} \in \mathbb{R}^d$ and $Y \in \mathbb{R}$.

In this setup, the intermediate threshold $Q(\tau_0)$, shape parameter γ and scale parameter σ in [\(4\)](#) may depend on covariates, and the extreme value approximation for the extreme conditional quantile becomes

$$Q_{\mathbf{x}}(\tau) \approx Q_{\mathbf{x}}(\tau_0) + \sigma(\mathbf{x}) \frac{\left(\frac{1-\tau}{1-\tau_0}\right)^{-\gamma(\mathbf{x})} - 1}{\gamma(\mathbf{x})}, \quad \tau > \tau_0. \quad (9)$$

The triple $(Q_{\mathbf{x}}(\tau_0), \sigma(\mathbf{x}), \gamma(\mathbf{x}))$ provides a model for the tail (that is above the probability level τ_0) of the conditional law of Y given $\mathbf{X} = \mathbf{x}$. An estimator of conditional extreme quantiles $\hat{Q}_{\mathbf{x}}(\tau)$ is obtained by plugging in estimators $(\hat{Q}_{\mathbf{x}}(\tau_0), \hat{\sigma}(\mathbf{x}), \hat{\gamma}(\mathbf{x}))$ in Equation (9).

In the next section we propose estimators for these three quantities. For estimation of the intermediate quantile $Q_{\mathbf{x}}(\tau_0)$, we outline how the existing method of quantile random forests can be applied. For $\sigma(\mathbf{x})$ and $\gamma(\mathbf{x})$ we develop new estimators based on a gradient boosting procedure that allows flexible regression functions with possibly many covariates.

3.2 Gradient boosting for extremes: gbex

For the estimation of the intermediate threshold, we fit the generalized random forest from Section 2.2 and then predict the conditional quantile $Q_{\mathbf{x}}(\tau_0)$. For prediction at the observed covariate values $\mathbf{x} = \mathbf{X}_1, \dots, \mathbf{X}_n$, we use out-of-bag estimation, denoted by $\hat{Q}_{\mathbf{X}_i}^{oob}(\tau_0)$. This means that only the trees for which the i th observation is out-of-bag are kept for the quantile estimation at $\mathbf{x} = \mathbf{X}_i$, i.e. trees based on sub-samples not containing the i -th observation. This is necessary to avoid giving too much weight to the i th observation when predicting at $\mathbf{x} = \mathbf{X}_i$. For a precise description of out-of-bag estimation we refer to Appendix B.

Once the generalized random forest is fitted to estimate the intermediate conditional quantile at probability level τ_0 , we define the exceedances of the data set $(\mathbf{X}_1, Y_1), \dots, (\mathbf{X}_n, Y_n)$ above the threshold as

$$Z_i = \left(Y_i - \hat{Q}_{\mathbf{X}_i}^{oob}(\tau_0) \right)_+, \quad i = 1, \dots, n,$$

so that $Z_i = 0$ whenever the value Y_i is below threshold. We assume that the intermediate threshold is high enough so that the exceedances can be modeled by the generalized Pareto distribution and the approximation of conditional quantiles (9) is good enough. Our

aim is to learn the conditional parameters $\theta(\mathbf{x}) = (\sigma(\mathbf{x}), \gamma(\mathbf{x}))$ based on the exceedances Z_1, \dots, Z_n . Following [Friedman \(2001\)](#) and [Friedman \(2002\)](#), we propose to use gradient boosting with a suitable objective function.

In absence of covariates, a standard way of estimating the GPD parameters $\theta = (\sigma, \gamma)$ is maximum likelihood method, which provides asymptotically normal estimators in the unconditional case with $\gamma > -1/2$ ([Smith, 1987](#)). Likewise, we use the negative log-likelihood, or equivalently the deviance of GPD distribution as the objective function of the gradient boosting procedure. Precisely, the deviance for an exceedance Z_i from a GPD distribution with parameters $\theta(\mathbf{X}_i) = (\sigma(\mathbf{X}_i), \gamma(\mathbf{X}_i))$ is given by

$$\ell_{Z_i}(\theta(\mathbf{X}_i)) = \left[(1 + 1/\gamma(\mathbf{X}_i)) \log \left(1 + \gamma(\mathbf{X}_i) \frac{Z_i}{\sigma(\mathbf{X}_i)} \right) + \log \sigma(\mathbf{X}_i) \right] \mathbb{I}_{Z_i > 0}. \quad (10)$$

Since the deviance depends on two parameters γ and σ , we need to build two sequences of trees, one for each parameter; [Friedman \(2001\)](#) proposes a similar strategy in multi-class classification where several sequences of trees are trained to learn the different class probabilities.

The gradient boosting algorithm starts with an initial estimate, which is given by the unconditional maximum likelihood estimator, that is, by setting $\theta(\mathbf{X}_i) \equiv \theta$ in (10):

$$\theta_0(\mathbf{x}) \equiv \underset{\theta}{\operatorname{argmin}} \sum_{i=1}^n \ell_{Z_i}(\theta). \quad (11)$$

The two sequences of gradient trees $(T_b^\sigma)_{1 \leq b \leq B}$ and $(T_b^\gamma)_{1 \leq b \leq B}$ are built recursively. We use the superscript $\delta \in \{\sigma, \gamma\}$ and the convenient notation $\theta = (\theta^\sigma, \theta^\gamma)$ to treat the two sequences simultaneously. Let $s \in (0, 1]$ denote a subsampling fraction. Sequentially for $b = 1, \dots, B$, we draw a random subset $S_b \subset \{1, \dots, n\}$ of size $[sn]$ and fit a pair of regression trees (T_b^σ, T_b^γ) to learn the gradient of the deviance on subsample S_b given by

$$r_{b,i}^\delta = \frac{\partial \ell_{Z_i}}{\partial \theta^\delta}(\theta_{b-1}(\mathbf{X}_i)), \quad i \in S_b, \delta \in \{\sigma, \gamma\}.$$

The regression tree T_b^δ is fitted on the sample $(\mathbf{X}_i, r_{b,i}^\delta)$, $i \in S_b$, by recursive binary splitting. Two further parameters are used to build the tree: the maximal depth D^δ gives the maximum number of splits between the root and a leaf in the tree; the minimal leaf size gives the minimum number of observations in each leaf. The leaves of the tree T_b^δ are denoted by $L_{b,j}^\delta$, $j = 1, \dots, J_b^\delta$, with J_b^δ the number of leaves.

Now that the tree T_b^δ is built, we need to update the value of parameter δ for each leaf such that the deviance is minimized. In theory this can be done by line search, that is, for leaf $L_{b,j}^\delta$, the updated value $\xi_{b,j}^\delta$ is obtained by minimizing the deviance, i.e.,

$$\xi_{b,j}^\delta = \underset{\xi}{\operatorname{argmin}} \sum_{\mathbf{X}_i \in L_{b,j}^\delta} \ell_{Z_i}(\theta_{b-1}(\mathbf{X}_i) + \xi e_\delta), \quad j = 1, \dots, J_b^\delta, \quad (12)$$

where $e_\sigma = (1, 0)$ and $e_\gamma = (0, 1)$ give the directions of the line search corresponding to parameters σ and γ , respectively. In practice the line search (12) can be computationally expensive and $\xi_{b,j}^\delta$ is approximated by a Newton–Raphson step

$$\tilde{\xi}_{b,j}^\delta = - \frac{\sum_{\mathbf{X}_i \in L_{b,j}^\delta} \frac{\partial \ell_{Z_i}}{\partial \theta^\delta}(\theta_{b-1}(\mathbf{X}_i))}{\sum_{\mathbf{X}_i \in L_{b,j}^\delta} \frac{\partial^2 \ell_{Z_i}}{\partial (\theta^\delta)^2}(\theta_{b-1}(\mathbf{X}_i))}.$$

The derivatives of the deviance are provided in Appendix C. Due to the instability of the derivatives of the GPD likelihood, we bound the absolute value of the Newton–Raphson step by 1 in order to mitigate the strong influence of extreme observations. We observe in practice that this results in better performance. This leads to the value

$$T_b^\delta(\mathbf{x}) = \sum_{j=1}^{J_b^\delta} \operatorname{sign}(\tilde{\xi}_{b,j}^\delta) \min(|\tilde{\xi}_{b,j}^\delta|, 1) \mathbb{I}_{\{\mathbf{x} \in L_{b,j}^\delta\}}. \quad (13)$$

for the gradient tree. The model $\theta_{b-1}(\mathbf{x})$ is then updated by

$$\theta_b^\delta(\mathbf{x}) = \theta_{b-1}^\delta(\mathbf{x}) + \lambda^\delta T_b^\delta(\mathbf{x}), \quad \delta \in \{\sigma, \gamma\}, \quad (14)$$

where the shrinkage parameters $\lambda^\sigma, \lambda^\gamma \in (0, 1)$ are called learning rates. They are used to slow down the dynamic since a shrunken version of the trees is added to the current model.

The final output for the estimated parameters is the gradient boosting model

$$\hat{\theta}^\delta(\mathbf{x}) = \theta_0^\delta + \lambda^\delta \sum_{b=1}^B T_b^\delta(\mathbf{x}), \quad \delta \in \{\sigma, \gamma\}. \quad (15)$$

In practice, the number of iterations B is an important parameter and its choice corresponds to a trade-off between bias and variance. The procedure is prone to overfitting as $B \rightarrow \infty$ and cross-validation is used to prevent this by early stopping; see Section 4.1 where we discuss the interpretation of the different tuning parameters and their selection in practice. We summarize the procedure for GPD modeling of exceedances in Algorithm 1 and the procedure for extreme quantile regression in Algorithm 2 in Appendix A. We shall refer to the developed algorithms as the **gbex** method. It combines the flexibility of gradient boosting with the extrapolation technique from extreme value theory.

4 Parameter tuning and interpretation

4.1 Parameter tuning

Our gradient boosting procedure for GPD modelling includes several parameters that need to be tuned properly for good results. We discuss in this section the interpretation of the different parameters and how to choose them. We introduce data driven choices based on cross validation for the most sensitive parameters and suggest sensible default values for the remaining parameters.

Algorithm 1 gbex boosting algorithm for GPD modeling

Input:

- θ_0 : the initial values of the parameters with default value as in (11);
- $(\mathbf{X}_i, Z_i)_{1 \leq i \leq n}$: data sample of exceedances above threshold;
- B : number of gradient trees;
- D^σ, D^γ : maximum tree depth for the gradient trees;
- $\lambda^\sigma, \lambda^\gamma$: learning rates for the update of the GPD parameters σ and γ respectively;
- s : subsampling fraction;
- $L_{min}^\sigma, L_{min}^\gamma$: minimum leaf size of the nodes in the trees.

Algorithm: For $b = 1, \dots, B$:

1. Draw a random subsample $S_b \subset \{1, \dots, n\}$ of size $[sn]$.
2. Compute the deviance derivatives on the subsample S_b :

$$r_{b,i}^\sigma = \frac{\partial \ell_{Z_i}}{\partial \sigma}(\theta_{b-1}(\mathbf{X}_i)) \quad \text{and} \quad r_{b,i}^\gamma = \frac{\partial \ell_{Z_i}}{\partial \gamma}(\theta_{b-1}(\mathbf{X}_i)), \quad i \in S_b.$$

3. Fit regression trees T_b^σ, T_b^γ that predict the gradients $r_{b,i}^\sigma$ and $r_{b,i}^\gamma$ as functions of the covariates \mathbf{X}_i on the sample $i \in S_b$; the trees are built with maximal depth (D^σ, D^γ) and minimal leaf size $(L_{min}^\sigma, L_{min}^\gamma)$; for the tree values, use the truncated Newton–Raphson rule (13).
4. Update the GPD parameters $\theta_b(\mathbf{x}) = (\hat{\sigma}_b(\mathbf{x}), \hat{\gamma}_b(\mathbf{x}))$ with learning rates $(\lambda^\sigma, \lambda^\gamma)$, i.e.,

$$\hat{\sigma}_b(\mathbf{x}) = \hat{\sigma}_{b-1}(\mathbf{x}) + \lambda^\sigma T_b^\sigma(\mathbf{x}) \quad \text{and} \quad \hat{\gamma}_b(\mathbf{x}) = \hat{\gamma}_{b-1}(\mathbf{x}) + \lambda^\gamma T_b^\gamma(\mathbf{x}).$$

Output: Conditional GPD parameters $(\hat{\sigma}(\mathbf{x}), \hat{\gamma}(\mathbf{x})) = (\hat{\sigma}_B(\mathbf{x}), \hat{\gamma}_B(\mathbf{x}))$.

4.1.1 Tree number B

The number of trees is the most important regularization parameter. The boosting procedure starts from a constant model, that is usually an underfit, and adds recursively trees that adapt the model to the data, leading eventually to an overfit.

We recommend repeated K -fold cross-validation based on the deviance for a data driven choice of B . Given a maximal tree number B_{max} and a division of the data set into K folds $\mathcal{D}_1, \dots, \mathcal{D}_K$, we repeatedly run the algorithm with B_{max} iterations on the data with one fold left-out and then compute the deviance on the left-out fold as a function of B . Adding up the deviances for the different folds, we obtain the cross-validation deviance. More formally, we define

$$\text{DEV}_{CV}(B) = \sum_{k=1}^K \sum_{i \in \mathcal{D}_k} \ell_{Z_i}(\hat{\theta}_B^{-\mathcal{D}_k}(\mathbf{X}_i)), \quad B = 0, \dots, B_{max}, \quad (16)$$

where $\hat{\theta}_B^{-\mathcal{D}_k}$ denotes the model with B trees trained on the data sample with the k th fold \mathcal{D}_k held out. Due to large values of the deviance on extreme observations, the cross-validation deviance is prone to fluctuations with respect to the partition into folds and we therefore recommend repeated cross-validation. A typical choice is $K = 5$ or 10 with 5 repetitions. The choice of B is then the minimizer of the cross-validation deviance.

4.1.2 Tree depth (D^σ, D^γ)

The gradient boosting algorithm outputs a sum of tree functions. The complexity of the model is therefore determined by the depth parameters D^σ and D^γ , also called interaction depths (see [Hastie et al., 2009](#), Section 10.11). A zero depth tree corresponds to a constant tree with no split, so that $D^\sigma = 0$ or $D^\gamma = 0$ yield models with constant scale or shape parameters, respectively. Since the extreme value index γ is notoriously difficult to estimate,

it is common in extreme value theory to assume a constant value $\gamma(\mathbf{x}) \equiv \gamma$ so that the case $D^\gamma = 0$ is particularly important. A tree with depth 1, also called a stump, makes only one single split on a single variable. As a result, $D^\sigma = 1$ (resp. $D^\gamma = 1$) corresponds to an additive model in the predictors for $\sigma(\mathbf{x})$ (resp. $\gamma(\mathbf{x})$). Trees with larger depth allow to introduce interaction effects between the predictors of order equal to the depth parameter. In practice, the depth parameter is quite hard to tune and we recommend to consider depth no larger than 3, also because interactions of higher order are difficult to interpret. Based on our experience, sensible default values are $D^\sigma = 2$ and $D^\gamma = 1$. But more interestingly, cross-validation can be used to select the depth parameters. The left panel of Figure 1 shows a typical cross-validation diagnostic in the context of the simulation study detailed in Section 5. Here $B_{max} = 500$ and depths parameter $(D^\sigma, D^\gamma) = (1, 0)$, $(1, 1)$, $(2, 1)$ and $(2, 2)$ are considered. The plot shows that sensible choices are $B \approx 200$ and $(D^\sigma, D^\gamma) = (1, 0)$ or $(1, 1)$ (more details given in Section 5). The histogram in the right panel shows that, depending on the randomly simulated sample, B typically lies in the range $[100, 250]$, where the deviance is relatively flat ($(D^\sigma, D^\gamma) = (1, 0)$ is fixed here).

4.1.3 Learning rates $(\lambda^\sigma, \lambda^\gamma)$

As usual in gradient boosting, there is a balance between the learning rate and the number of trees. As noted in Ridgeway (2007), multiplying the learning rate by 0.1 roughly requires 10 times more trees for a similar result. It is common to fix the learning rate to a small value, typically 0.01 or 0.001, and to consider the tree number as the main parameter. Since in our case we have two parallel gradient boosting procedures with different learning rates, we reparameterize them as $(\lambda_{scale}, \lambda_{ratio}) = (\lambda^\sigma, \lambda^\sigma / \lambda^\gamma)$. The balance described above is expressed between B and λ_{scale} and we propose the default $\lambda_{scale} = 0.01$, leaving the number

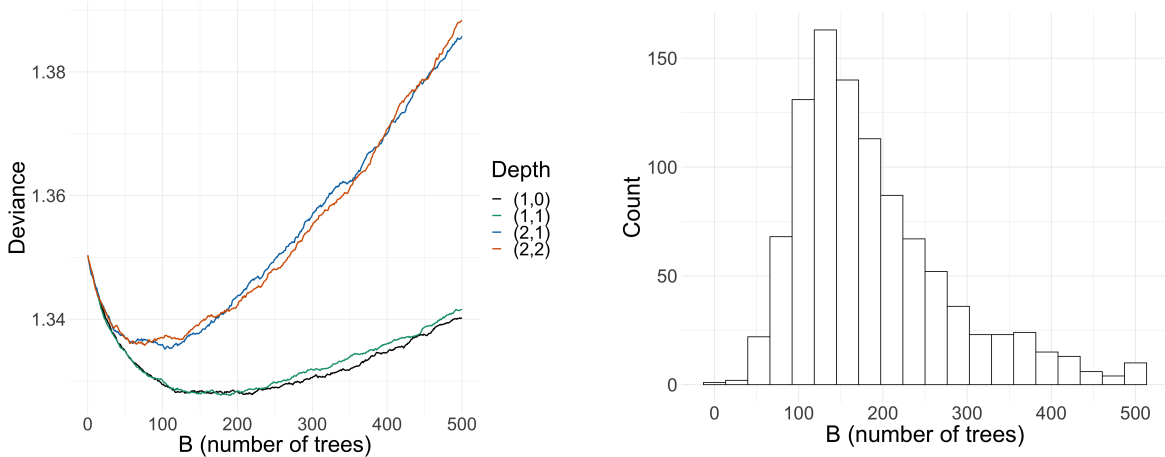


Figure 1: Left panel: cross-validation deviance given by (16) against B for one random sample and depth $(D^\sigma, D^\gamma) = (1, 0)$, $(1, 1)$, $(2, 1)$ and $(2, 2)$. Right panel: selected values of B for 1000 samples when $(D^\sigma, D^\gamma) = (1, 0)$ is fixed. The design of the simulation study is Model 1 described in Section 5.

of trees B as the primary parameter. The ratio of the learning rates is important as γ generally requires stronger regularization than σ and ranges on smaller scales. Therefore it is natural to choose $\lambda_{ratio} > 1$. Often a sensible default for λ_{ratio} falls in between 5 and 10.

4.1.4 Remaining tuning parameters

The minimum leaf sizes $L_{min}^\sigma, L_{min}^\gamma$ and subsample fraction s play the role of regularization parameters. The minimum leaf size makes sure that the splits do not try to isolate a single high observation of the gradient and that the leaves contain enough observations so that averaging provides a smoother gradient. Subsampling ensures that different trees are fitted on different sub-samples, mitigating the correlation between trees; see [Friedman \(2002\)](#) and [Hastie et al. \(2009, Section 10.12.2\)](#) for further discussion on the regularization effect of

subsampling. In practice, we do not recommend to optimize these parameters but rather to use the sensible default parameters $L_{min}^\sigma = L_{min}^\gamma = \max(10, n/100)$ and $s = 75\%$.

The parameter τ_0 stands for the probability level of the intermediate quantile used as threshold. Threshold selection is a long standing problem in extreme value theory (e.g., [Dupuis, 1999](#); [Drees et al., 2020](#)). A higher threshold yields a better approximation by the GPD distribution but fewer exceedances, leading to reduced bias and higher variance. Some guidelines for threshold selection in practice are provided in [Section 6](#), where we present an application to precipitation forecast statistical post-processing.

4.2 Tools for model interpretation

Contrary to a single tree, boosting models that aggregate hundreds or thousands of trees are difficult to represent but diagnostic plots are available to ease the interpretation. We briefly discuss variable importance and partial dependence plots, which are straightforward modifications to our framework of the tools detailed in [Hastie et al. \(2009, Section 10.13\)](#).

4.2.1 Variable importance

Boosting is quite robust to the curse of dimensionality and often provides good results even in the presence of high dimensional predictors and noise variables. Understanding which predictors are the most important is crucial for model interpretation. Variable importance is used for this purpose and we discuss here the permutation score and the relative importance.

The permutation score helps to evaluate the impact of a predictor on the model deviance and is not specific to boosting. The relation between a predictor and the response is disturbed by shuffling the values of this predictor and measuring the difference in the

deviance before and after shuffling. More precisely, for predictor X_j , we define

$$I(X_j) = \sum_{i=1}^n \ell_{Z_i} \left(\hat{\theta} \left(\mathbf{X}_i^{(j)} \right) \right) - \sum_{i=1}^n \ell_{Z_i} \left(\hat{\theta} \left(\mathbf{X}_i \right) \right), \quad (17)$$

where $\hat{\theta}$ is the estimator given in (15) and $\mathbf{X}_1^{(j)}, \dots, \mathbf{X}_n^{(j)}$ denote the same input vectors as $\mathbf{X}_1, \dots, \mathbf{X}_n$ except that the j th components are randomly shuffled. A large permutation score $I(X_j)$ indicates a strong effect of X_j in the boosting model. Since the scores are relative, it is customary to assign to the largest the value of 100 and scale the others accordingly.

The relative importance is specific to tree based methods such as boosting or random forests and uses the structure of the trees in the model. It is discussed for instance in [Hastie et al. \(2009, Section 10.13.1\)](#). Recall that during the construction of the trees, the splits are performed so as to minimize the residual sum of squares (RSS) of the gradient and each split causes a decrease in the RSS. The more informative splits are those causing a large decrease in the RSS. The relative importance of a given variable X_j is obtained by considering all the splits due to this variable in the sequence of trees, and by summing up the decrease in RSS due to those splits. Because we have two sequences of trees, we compute relative importance of variable X_j in the estimation of σ and γ separately by considering the sequence of trees (T_b^σ) and (T_b^γ) respectively.

4.2.2 Partial dependence plot

Once the most relevant variables have been identified, the next attempt is to understand the dependence between the predictors and the response. Partial dependence plots offer a nice graphical diagnostic of the partial influence of a predictor X_j on the outputs $\hat{\sigma}(\mathbf{x})$, $\hat{\gamma}(\mathbf{x})$ or $\hat{Q}_{\mathbf{x}}(\tau)$; see [Hastie et al. \(2009, Section 10.13.2\)](#). The partial dependence plot for

$\hat{\sigma}$ with respect to X_j is the graph of the function $x \mapsto \frac{1}{n} \sum_{i=1}^n \hat{\sigma}(\mathbf{X}_i^{-j,x})$, where the vector $\mathbf{X}_i^{-j,x}$ is equal to \mathbf{X}_i except that the j th component has been replaced by x . Notice that dependence between the predictors is not taken into account so that this is not an estimate of $\mathbb{E}[\hat{\sigma}(\mathbf{X}) \mid X_j = x]$, except if X_j is independent of the other predictors. In the particular case when an additive model is built, i.e., $D^\sigma = 1$, the partial dependence plot with respect to X_j is equal to the effect of the variable X_j up to an additive constant. Partial dependence plots with respect to several covariates can be defined and plotted similarly, at least in dimension 2 or 3.

5 Simulation studies

To demonstrate the performance of our method, we conduct two numerical experiments. We generate n independent samples with d covariates $\mathbf{X} = (X_1, \dots, X_d)$ distributed from an independent uniform distribution on $[-1, 1]^d$, with $(n, d) = (2000, 40)$ or $(5000, 10)$, depending on the complexity of the model. We aim to estimate the conditional quantile function $Q_{\mathbf{x}}(\tau)$ corresponding to extreme probability levels $\tau \in \{0.99, 0.995, 0.9995\}$. We choose the level $\tau_0 = 0.8$ for the intermediate quantile and it is worthwhile to note that the effective sample size $n(1 - \tau_0)$ for the gradient boosting step is then only 400 for $n = 2000$.

The local smoothing based methods mentioned in the introduction ([Gardes and Stupfler, 2019](#); [Daouia et al., 2013](#)) become cumbersome in our simulation setting because of the sparsity of data in high dimension. We compare our `gbex` method to two quantile regression approaches, the quantile regression forest (`qrf`) from [Meinshausen \(2006\)](#) and the generalized random forest (`grf`) from [Athey et al. \(2019\)](#). Moreover, we consider two existing methods from extreme value theory that use GPD modeling of the exceedances. One is

the classical estimator of extreme quantile without using covariates, thus $\gamma(\mathbf{x}) \equiv \gamma$ and $\sigma(\mathbf{x}) \equiv \sigma$, which we call the **constant** method. The other one is the **evgam** method of [Youngman \(2019\)](#) that assumes generalized additive models for $\gamma(\mathbf{x})$ and $\sigma(\mathbf{x})$.

To evaluate the performance over the full predictor domain $[-1, 1]^d$ we consider the integrated squared error (ISE) defined for a fixed quantile level τ and the i th replication of the data set by

$$\text{ISE}_i = \int_{[-1, 1]^d} \left(\hat{Q}_{\mathbf{x}}^{(i)}(\tau) - Q_{\mathbf{x}}(\tau) \right)^2 d\mathbf{x}, \quad (18)$$

where $\hat{Q}_{\mathbf{x}}^{(i)}(\tau)$ is the quantile estimated from the model. We use a Halton sequence, a low discrepancy quasi-random sequence (e.g., [Niederreiter, 1992](#), p. 29), in order to efficiently evaluate the high dimensional integral in the ISE computation. Averaging over the $R = 1000$ replications, we obtain the mean integrated squared error (MISE).

Our first model is designed to check robustness of the methods against noise variables. This model is constructed in a similar way as the example studied in [Athey et al. \(2019, Section 5\)](#) and it has a predictor dimension of $d = 40$, of which one covariate is signal and the remaining are noise variables.

- **Model 1:** Given $\mathbf{X} = \mathbf{x} \in \mathbb{R}^{40}$, Y follows a Student's t -distribution with 4 degrees of freedom and scale

$$\text{scale}(\mathbf{x}) = 1 + \mathbb{I}(x_1 > 0).$$

This is a heavy tailed model where the GPD approximation has a constant shape parameter $\gamma(\mathbf{x}) \equiv 1/4$ and the scale parameter is a step function in X_1 . More precisely, $\sigma(\mathbf{x}) = \sigma(\tau_0)(1 + \mathbb{I}(x_1 > 0))$ where $\sigma(\tau_0)$ is a multiplicative constant depending on the threshold parameter τ_0 .

In our second model, we consider a more complex response surface where both the scale and shape parameters depend on the covariates and interactions of order 2 are introduced.

- **Model 2:** Given $\mathbf{X} = \mathbf{x} \in \mathbb{R}^{10}$, Y follows a Student's t -distribution with degree of freedom $\text{df}(\mathbf{x})$ depending on x_1 through

$$\text{df}(\mathbf{x}) = 7(1 + \exp(4x_1 + 1.2))^{-1} + 3,$$

and scale parameter $\text{scale}(\mathbf{x})$ depending on (x_1, x_2) through

$$\text{scale}(\mathbf{x}) = 1 + 6\varphi(x_1, x_2),$$

where φ denotes the density function of a bivariate normal distribution with standard normal margins and correlation 0.9. The numerical constants are chosen so that the GPD approximation of Y given $\mathbf{X} = \mathbf{x}$ has parameters $\gamma(\mathbf{x}) = 1/\text{df}(\mathbf{x})$ in the range $[0.10, 0.33]$ for $\mathbf{x} \in [-1, 1]^d$, $d = 10$.

5.1 Tuning parameters and cross validation

We generate samples of size $n = 2000$ and 5000 , respectively from Model 1 and Model 2. We set the following tuning parameters for **gbex**: the learning rate $\lambda_{\text{scale}} = 0.01$ and the sample fraction $s = 75\%$ for both models; $\lambda_{\text{ratio}} = 15$ for Model 1 and $\lambda_{\text{ratio}} = 7$ for Model 2.

As discussed in Section 4.1, the number of trees B is the most important regularization parameter and the depth parameters (D^σ, D^γ) determine the complexity of the fitted model. Therefore, we investigate how these tuning parameters influence the performance of our estimator in terms of MISE. Figure 2 shows the results for Model 1 (left panel) and for Model 2 (right panel). The curves represent the MISE of **gbex** as a function of B for

various depth parameters (D^σ, D^γ) . The right panel clearly shows that for Model 2 the choice $(D^\sigma, D^\gamma) = (1, 1)$ does not account for the model complexity adequately, which leads to a high MISE. Indeed, boosting with depth one tries to fit an additive model but the scale parameter of Model 2 depends on (X_1, X_2) in a non-additive way. On the other hand, for Model 1, which is an additive model with the optimal depth $(D^\sigma, D^\gamma) = (1, 0)$, the curves suggest that assuming unnecessary complexity of the model might lead to suboptimal behavior of the estimator: the choice $(2, 1)$ yields higher MISE than the other two choices and the MISE stays low for a shorter range of B . In general, higher depths help the model to adapt the data faster but then overfitting is prone to occur more rapidly when B increases. The horizontal dashed lines in Figure 2 represent the resulting MISE of our estimator when B is chosen via cross-validation with deviance loss given in (16), with $K = 5$ folds and 10 replications. The plots confirm that the data driven choice of B results in near optimal MISE for fixed depth parameters (with dashed horizontal lines close to the minimum of the curve with the same color). We additionally apply cross-validation to select both B and (D^σ, D^γ) simultaneously. The resulting MISE is represented by the black dashed line, which is very close to the minimum of all the dashed lines. Overall, the results confirm the good performance of the proposed cross-validation procedure.

For the rest of the simulation study, we set $(D^\sigma, D^\gamma) = (1, 1)$ for Model 1 and $(D^\sigma, D^\gamma) = (3, 1)$ for Model 2 and choose B with cross-validation.

5.2 Comparison with different methods

The comparison of our **gbex** method to the other three approaches **qrf**, **grf** and **constant**, is presented in Figure 3. The results for Model 1 and Model 2 are given in the first and second row, respectively. For the probability level $\tau = 0.99, 0.99$ and 0.9995 in the left,

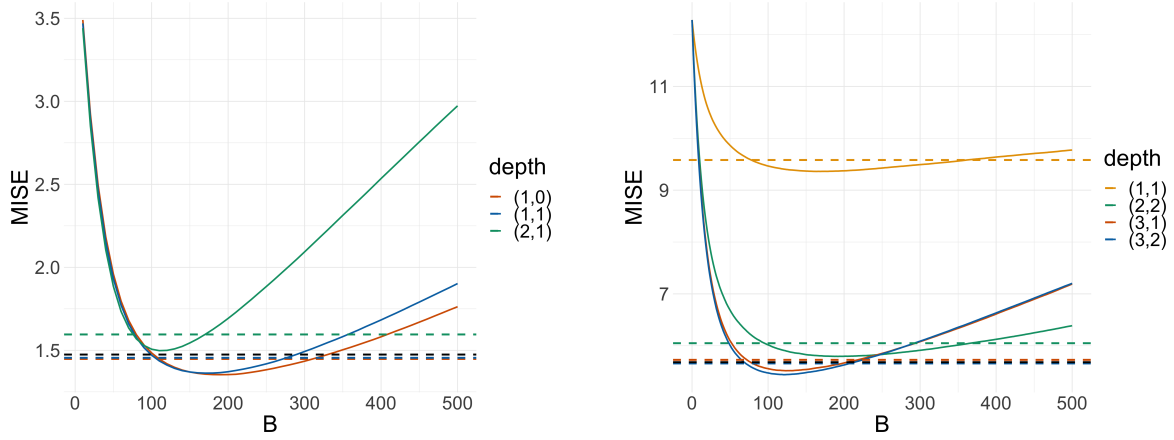


Figure 2: The MISE for Model 1 (left panel) and Model 2 (right panel) of the **gbex** extreme quantile estimator with probability level $\tau = 0.995$ as a function of B for various depth parameters (curves); the MISE of the **gbex** estimator with adaptive choice of B for various depth parameters (horizontal dashed lines); the MISE of the **gbex** estimator with both tree number and depth parameters selected by cross-validation (black dashed line).

middle and right column, the figure shows the boxplots of ISE defined in (18) and the MISE represented by the vertical black line. The MISE grows as the probability level increases for all methods, however **gbex** clearly outperforms the other three approaches with a much smaller MISE and a much lower variation of ISE. When the probability level τ is close to or larger than $(1 - 1/n)$ (right column), both **grf** and **qrf** lead to extremely large ISE outliers so that the ISE mean is larger than the third quartile (black line outside the box). Some extreme outliers of ISE are left out of the boxplots to have a clear comparison.

Because Model 2 does not satisfy the additive model assumption of **evgam**, the comparison between **evgam** and **gbex** is based on data generated from Model 1 only. Figure 4 presents the ISE and MISE of **evgam** and **gbex** for probability level $\tau = 0.995$. To have a

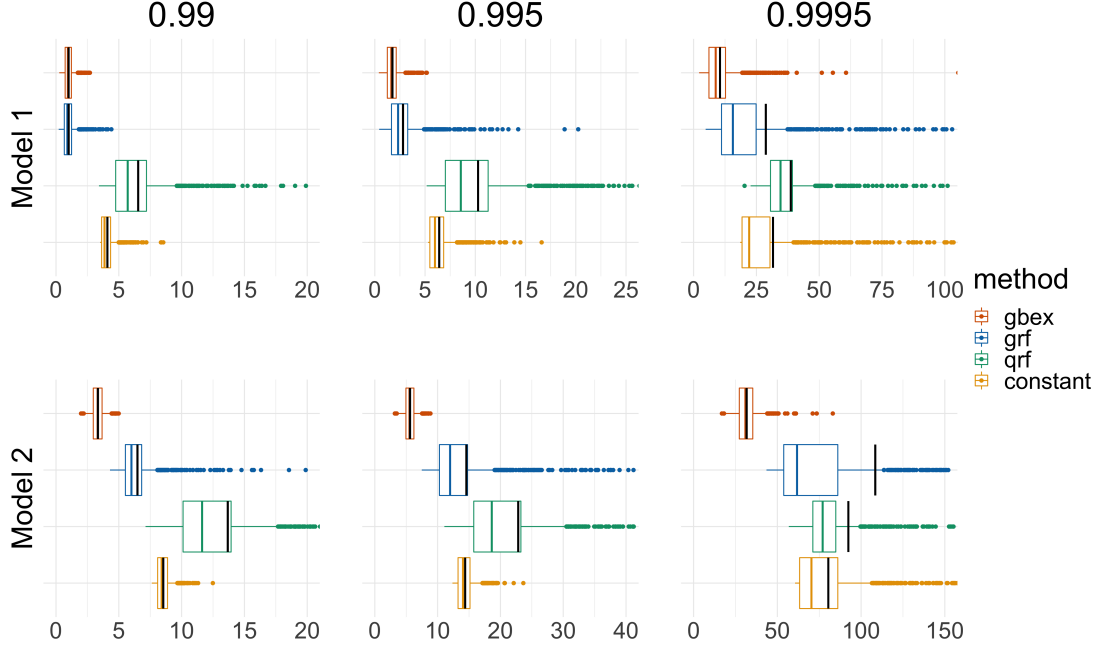


Figure 3: Boxplot of ISE based on 1000 replications for the four quantile estimators (**gbex**, **grf**, **qrf** and **constant**) at different probability levels $\tau = 0.99$ (left), 0.995 (middle) and 0.9995 (right) for Model 1 (top) and Model 2 (bottom). Some outliers of **grf** and **qrf** are left out for a clearer comparison. The black vertical lines indicate the MISE.

fair comparison, we use the same forest based estimation of quantile $\hat{Q}_{\mathbf{x}}(\tau_0)$ for the intermediate threshold. Because of the computational burden and numerical instability of **evgam** in high dimensions, we have restricted the dimension to $d \leq 10$ for this method, while **gbex** is still considered with $d = 40$. For **evgam**, the boxplots show a steady increase of the MISE with respect to the dimension and we can see that the MISE of **gbex** with $d = 40$ is similar to the MISE of **evgam** with $d = 4$. This clearly demonstrates the robustness of **gbex**

against the curse of dimensionality and noise variables, which is a prominent advantage of tree based methods.

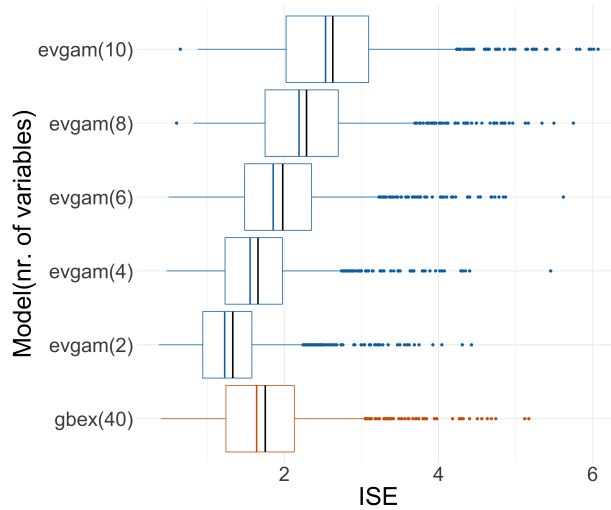


Figure 4: Boxplots of ISE based on 1000 replications for **evgam** estimator in dimension $d = 2, 4, 6, 8, 10$ (blue) and **gbex** estimator in dimension $d = 40$ (red) at probability levels $\tau = 0.995$. The vertical black lines indicate the MISE.

5.3 Diagnostic plots

We finally look at the model interpretation diagnostics. Figure 5 shows the permutation importance scores defined in (17) for both models, based on 1000 replications. The boxplots clearly show that this score is able to identify the signal variable(s). Note that there are 39 noise variables for Model 1 and 8 for Model 2. The scores of the noise variables behave all similarly and only a limited number are displayed. For Model 2, the permutation score is higher for X_1 than for X_2 , due to the fact that X_1 contributes to both shape and scale

functions while X_2 only contributes to the scale function.

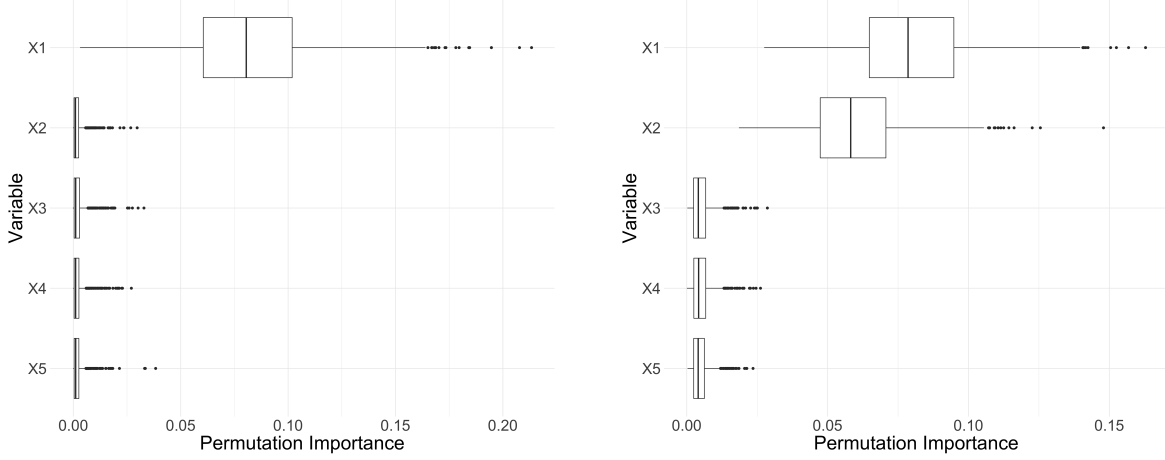


Figure 5: Boxplots of permutation scores defined in (17) for X_j , $j = 1, \dots, 5$, based on 1000 samples. Left panel: Model 1, where only X_1 contains signal. Right panel: Model 2, where only X_1 and X_2 contain signal.

The left panel of Figure 6 presents a typical partial dependence plot (Section 4.2) for $\hat{\sigma}$ based on one random sample from Model 1. This plot clearly suggests that $\hat{\sigma}$ is a step function of X_1 and does not depend on the noise variables. The partial dependence plot for $\hat{\gamma}$ indicates that the shape does not change with respect to any of the covariates. For this model, the partial dependence plots are in perfect agreement with the simulation design. For Model 2, the left panel of Figure 7 shows the partial dependence plot of the scale parameter with respect to X_1 and X_2 . We see that the model detects the right pattern of larger values on the diagonal and in the center. The right panel shows that the model identifies the impact of X_1 on the shape parameter while the partial dependence plot of the other variables is fairly constant, again in agreement with the simulation design.

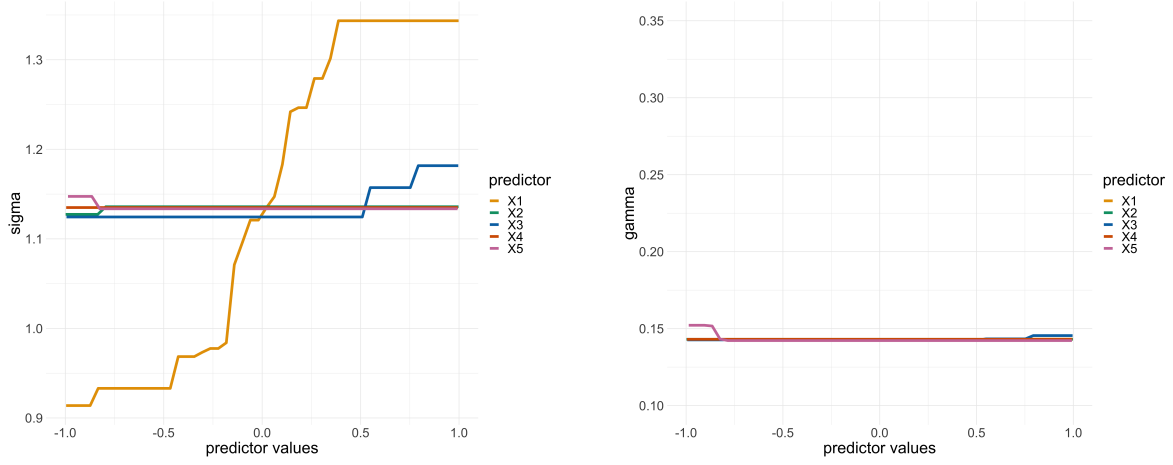


Figure 6: Partial dependence plots of $\hat{\sigma}$ (left panel) and of $\hat{\gamma}$ (right panel) with respect to X_j , $j = 1, \dots, 5$, based on one random sample of Model 1.

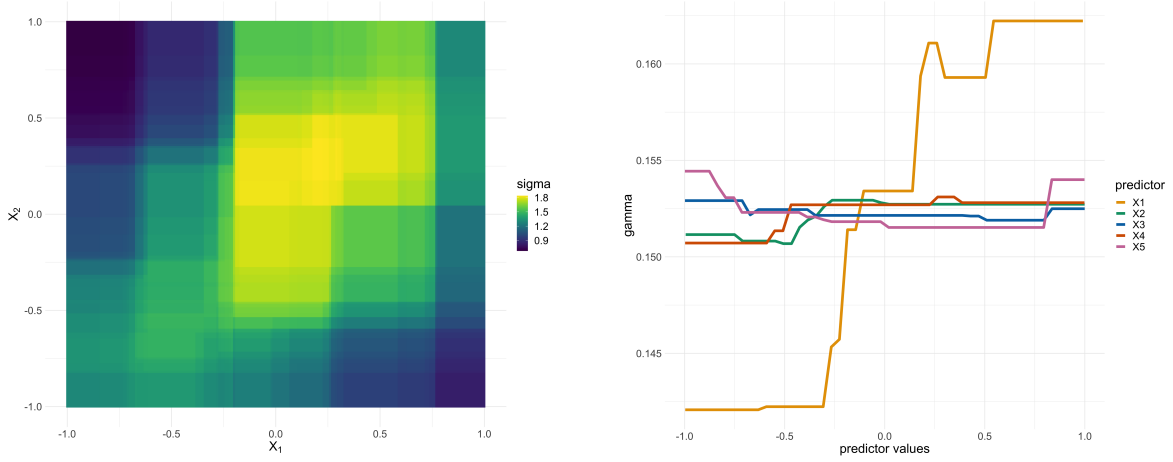


Figure 7: Left panel: partial dependence plots of $\hat{\sigma}$ with respect to (X_1, X_2) . Right panel: partial dependence plot of $\hat{\gamma}$ with respect to X_j , $j = 1, \dots, 5$. Both experiments corresponds to one random sample of Model 2.

6 Application to precipitation forecast

Extreme precipitation events can have disruptive consequences on our society. Accurate predictions are vital for taking preventive measures such as pumping water out of the system to prevent flooding. We apply our `gbex` method to predict extreme quantiles of daily precipitation using the output of numerical weather prediction (NWP) models.

Weather forecasts rely on NWP models that are based on non-linear differential equations from physics describing the atmospheric flow. The solutions to these equations with respect to initial conditions and parametrizations of unresolved processes form a forecast that is deterministic in nature. Introducing uncertainty in these initializations yields an ensemble forecast that consists of multiple members. In this application, we use the ensemble forecast from the European Centre for Medium-Range Weather Forecasts (ECMWF) as covariates in `gbex` to predict the daily precipitation. Using NWP output for further statistical inference to improve forecasts is known as statistical post-processing.

6.1 Precipitation Data

Our data set consists of ECMWF ensemble forecasts of daily accumulated precipitation and the corresponding observations at seven meteorological stations spread across the Netherlands (De Bilt, De Kooy, Eelde, Schiphol, Maastricht, Twente and Vlissingen)¹. We use about 9 years of data, from January 1st, 2011, until November 30th, 2019, with sample size $n = 3256$. We fit separate models for each station with response variable Y equal to the observed precipitation at the station between 00 UTC and 24 UTC.

¹Observed daily precipitation can be obtained from

<http://projects.knmi.nl/klimatologie/daggegevens/selectie.cgi>

As for the covariates, we use ECMWF ensemble forecasts of daily accumulated precipitation that is computed the day before at 12UTC. The ensemble forecast contains 51 members. For efficiency, we use two summary statistics, namely the standard deviation of the ensemble members and the upper order statistics (the maximum of the ensemble members). Because most part of the Netherlands is flat and the distance between stations is not large, we include the ensemble summary statistics of all stations as covariates for the model of each station. To account for seasonality, we additionally consider the sine and cosine with a period of 365 for the day of the year. The total covariate dimension is $d = 7 \times 2 + 2 = 16$, for each model. We denote our data as $(Y_i^{(l)}, \mathbf{X}_i)$, where $\mathbf{X}_i \in \mathbb{R}^{16}$, $i = 1, \dots, n = 3256$ and $l = 1, \dots, 7$. For station l , we apply the **gbex** Algorithm 2 to $\{(Y_i^{(l)}, \mathbf{X}_i), i = 1, \dots, n\}$ to obtain estimates of $Q_{\mathbf{X}}^{(l)}(\tau)$.

6.2 Model fitting

For model fitting, we have observed in a preliminary analysis that the output is sensitive to the initial value of (γ, σ) and we propose a specific strategy that provides better results than the default initialization. We consider a common initial value for the shape γ for all the stations and different initial values of σ for the different stations, which leads to $\theta_0 = (\gamma, \sigma_1, \dots, \sigma_7)$. More precisely, we obtain the initial values by optimizing the log-likelihood function

$$L(\theta_0) = \sum_{l=1}^7 \sum_{i=1}^n \left[(1 + 1/\gamma) \log \left(1 + \gamma \frac{Y_i^{(l)} - c}{\sigma_l} \right) + \log \sigma_l \right] \mathbb{I}_{\{Y_i^{(l)} - c > 0\}},$$

where c is a large threshold chosen such that the estimate of γ becomes stable.

We apply **gbex** as detailed in Algorithm 2 with $\tau_0 = 0.8$ for each model. We choose all tuning parameters except for B to be the same for the seven models, in such a way to achieve

the overall best combined deviance score for all stations. This prevents overfitting for a specific station and it results in the following choices: $(D^\sigma, D^\gamma) = (2, 1)$, $(\lambda_{scale}, \lambda_{ratio}) = (0.01, 12)$, $s = 50\%$, and $(L_{min}^\sigma, L_{min}^\gamma) = (15, 45)$. The optimal B for each station is then chosen as the minimizer of the cross-validated deviance; see Figure 11 in Appendix D. Figure 12 in Appendix D shows that the resulting covariate-dependent GPD model fits the data well at all stations, and in particular it outperforms the `constant` model.

6.3 Results

We first look into the variable importance scores for the fitted models and focus on the relative importance to understand which variables affect the scale and shape parameters, respectively. Figure 8 shows the relative importance for γ and σ . It is interesting to note that for the shape γ , the `day of year` is the most important variable in six out of seven models. This motivates to investigate the seasonality pattern in the extreme precipitation. The partial dependence plots of $\hat{\gamma}^{(l)}$ (left panel) and $\hat{Q}_{\mathbf{X}}^{(l)}(0.995)$ (right panel) with respect to the `day of year` are presented in Figure 9 for all stations. They indicate that the tail of the precipitation is heavier in summer and autumn than in winter and spring. The curves in the left panel resemble step functions and higher values of $\hat{\gamma}$ correspond to June, July and August for five stations. For the other two stations Twente and Vlissingen, it is shifted towards autumn.

Another relevant question concerns the contribution of ensemble statistics of other stations in forecasting the extreme precipitation of a specific location. To this end, we add the permutation scores of ensemble standard deviation and ensemble upper order statistics per station, resulting in seven scores for each model. We then normalize these scores such that the maximum score is 100. The results for three stations are visualized in Figure 10.

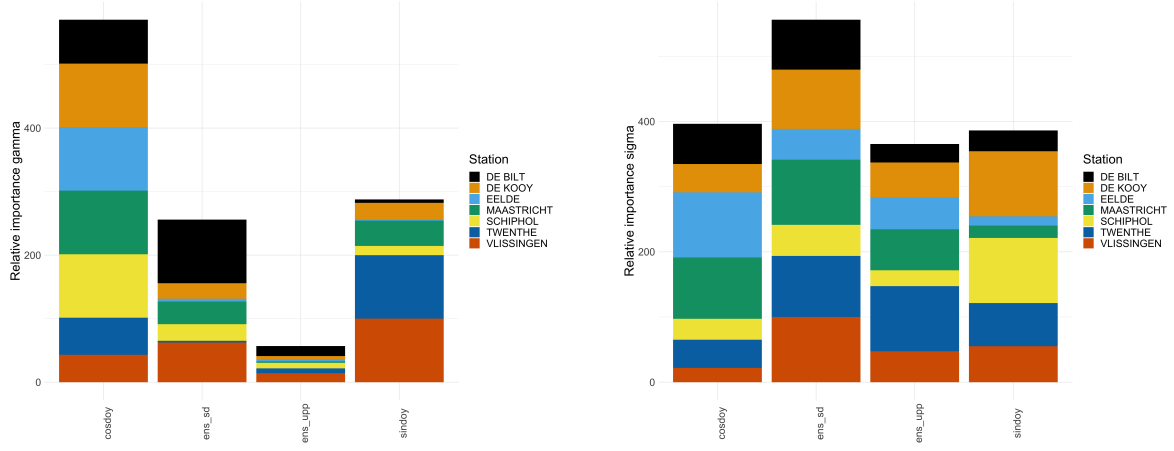


Figure 8: Relative variable importance score for γ (left) and σ (right). For each model, the scores are normalized such that the maximum score is 100.

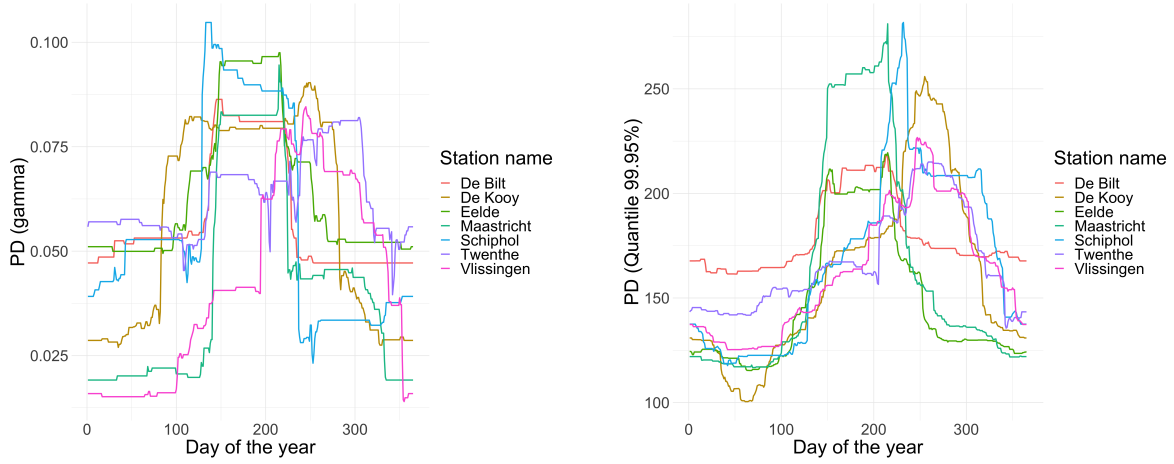


Figure 9: Partial dependence plots of $\hat{\gamma}^{(l)}$ (left panel) and $\hat{Q}_{\mathbf{X}}^{(l)}(0.995)$ (right panel, in mm) with respect to day of year.

First, quite surprisingly, when forecasting the extreme precipitation at Schiphol (left plot), the ensemble forecast relies on the information from Vlissingen and De Kooy even more

than the information at Schiphol, which might be explained by a coastal effect. Similarly, the model at De Bilt (middle plot) uses the information from Schiphol and Vlissingen. For other stations like Eelde (right plot), the own information of the station is the most important. The maps of the other four stations (De Kooy, Maastricht, Vlissingen and Twente) are very similar to that of Eelde.

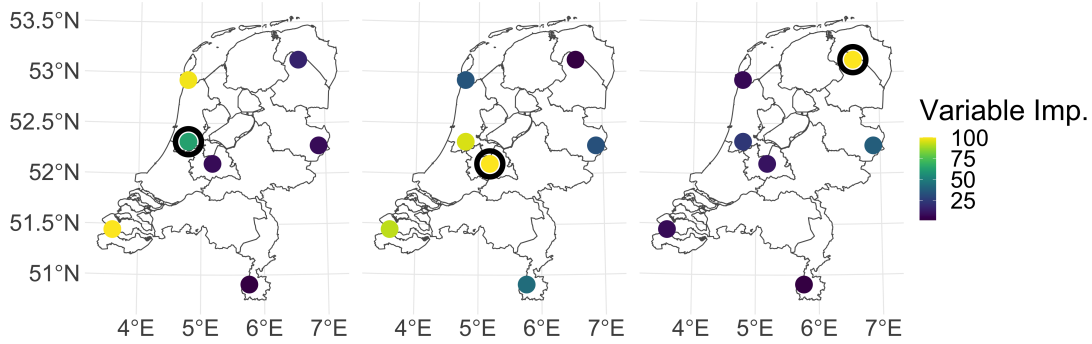


Figure 10: Normalized permutation scores of ensemble statistics per location for four models: Schiphol (left), De Bilt (middle), Eelde (right). The black circle indicates the station for which the model is fitted. From North to South, the stations are: Eelde, De Kooy, Twente, Schiphol, De Bilt, Vlissingen, Maastricht.

References

- Athey, S., Tibshirani, J., Wager, S., et al. (2019). Generalized random forests. *The Annals of Statistics*, 47(2):1148–1178.
- Balkema, A. A. and de Haan, L. (1974). Residual life time at great age. *The Annals of Probability*, 2(5):792–804.
- Breiman, L. (2001). Random forests. *Machine learning*, 45(1):5–32.

- Chavez-Demoulin, V. and Davison, A. (2005). Generalized additive modelling of sample extremes. *Journal of the Royal Statistical Society, series C*, 54.
- Chernozhukov, V. (2005). Extremal quantile regression. *Ann. Statist.*, 33(2):806–839.
- Daouia, A., Gardes, L., and Girard, S. (2013). On kernel smoothing for extremal quantile regression. *Bernoulli*, 19(5B):2557–2589.
- Davison, A. and Smith, R. (1990). Models for exceedances over high threshold. *Journal of the Royal Statistical Society, series B*, 52.
- Drees, H., Janßen, A., Resnick, S. I., and Wang, T. (2020). On a minimum distance procedure for threshold selection in tail analysis. *SIAM Journal on Mathematics of Data Science*, 2(1):75–102.
- Dupuis, D. J. (1999). Exceedances over high thresholds: A guide to threshold selection. *Extremes*, 1(3):251–261.
- Farkas, S., Lopez, O., and Thomas, M. (2019+). Cyber claim analysis through generalized pareto regression trees with applications to insurance pricing and reserving. Preprint <https://hal.archives-ouvertes.fr/hal-02118080>.
- Friedman, J. H. (2001). Greedy function approximation: a gradient boosting machine. *Annals of statistics*, pages 1189–1232.
- Friedman, J. H. (2002). Stochastic gradient boosting. *Computational statistics & data analysis*, 38(4):367–378.
- Gardes, L. and Stupfler, G. (2019). An integrated functional Weissman estimator for conditional extreme quantiles. *REVSTAT*, 17(1):109–144.
- Hastie, T., Tibshirani, R., and Friedman, J. (2009). *The elements of statistical learning*. Springer Series in Statistics. Springer, New York, second edition. Data mining, inference, and prediction.
- Koenker, R. (2005). *Quantile regression*, volume 38 of *Econometric Society Monographs*. Cambridge University Press, Cambridge.
- Koenker, R. and Bassett Jr, G. (1978). Regression quantiles. *Econometrica: journal of the Econometric Society*, pages 33–50.

- Meinshausen, N. (2006). Quantile regression forests. *Journal of Machine Learning Research*, 7(Jun):983–999.
- Niederreiter, H. (1992). *Random number generation and quasi-Monte Carlo methods*, volume 63 of *CBMS-NSF Regional Conference Series in Applied Mathematics*. Society for Industrial and Applied Mathematics (SIAM), Philadelphia, PA.
- Pickands III, J. (1975). Statistical inference using extreme order statistics. *Ann. Statist.*, 3(1):119–131.
- Ridgeway, G. (2007). Generalized boosting models: a guide to the gbm package. URL <https://cran.r-project.org/web/packages/gbm/vignettes/gbm.pdf>.
- Smith, R. L. (1987). Estimating tails of probability distributions. *Ann. Stat.*, 15:1174–1207.
- Velthoen, J., Cai, J.-J., Jongbloed, G., and Schmeits, M. (2019). Improving precipitation forecasts using extreme quantile regression. *Extremes*, 22(4):599–622.
- Wager, S. and Athey, S. (2018). Estimation and inference of heterogeneous treatment effects using random forests. *Journal of the American Statistical Association*, 113(523):1228–1242.
- Wang, H. and Tsai, C.-L. (2009). Tail index regression. *Journal of the American Statistical Association*, 104(487):1233–1240.
- Wang, H. J., Li, D., and He, X. (2012). Estimation of high conditional quantiles for heavy-tailed distributions. *Journal of the American Statistical Association*, 107(500):1453–1464.
- Youngman, B. D. (2019). Generalized additive models for exceedances of high thresholds with an application to return level estimation for u.s. wind gusts. *Journal of the American Statistical Association*, 114(528):1865–1879.

A Algorithms

Algorithm 2 gbex algorithm for extreme quantile prediction

Input:

- $(\mathbf{X}_i, Y_i)_{1 \leq i \leq n}$: data sample;
- τ_0 : probability level for the threshold;
- τ : probability level for the prediction such that $\tau > \tau_0$;
- parameters of the gbex boosting algorithm for GPD modeling of exceedances (Algorithm 1).

Algorithm:

1. Fit a quantile regression forest to the sample $(\mathbf{X}_i, Y_i)_{1 \leq i \leq n}$ that provides estimates $\hat{Q}_{\mathbf{x}}(\tau_0)$ of the conditional quantiles of order τ_0 .
2. Compute the exceedances $Z_i = (Y_i - \hat{Q}_{\mathbf{X}_i}^{oob}(\tau_0))_+$, $1 \leq i \leq n$, where $\hat{Q}_{\mathbf{X}_i}^{oob}(\tau_0)$ denotes the out-of-bag estimates of the conditional quantile at $\mathbf{x} = \mathbf{X}_i$.
3. Let $I = \{i : Z_i > 0\}$ be the index set of positive exceedances and run Algorithm 1 on the data set $(\mathbf{X}_i, Z_i)_{i \in I}$ to estimate the GPD parameters $(\hat{\sigma}(\mathbf{x}), \hat{\gamma}(\mathbf{x}))$.

Output: Estimation of the extreme conditional quantile

$$\hat{Q}_{\mathbf{x}}(\tau) = \hat{Q}_{\mathbf{x}}(\tau_0) + \hat{\sigma}(\mathbf{x}) \frac{\left(\frac{1-\tau}{1-\tau_0}\right)^{-\hat{\gamma}(\mathbf{x})} - 1}{\hat{\gamma}(\mathbf{x})}.$$

B Generalized random forest for quantile regression

We briefly describe the generalized random forest by [Wager and Athey \(2018\)](#) in the specific case of quantile regression; more details and theoretical results can be found in the original paper. Similar to Breiman’s random forests ([Breiman, 2001](#)), three different mechanisms are at play in the generalized random forests (GRF): i) resampling of the original data set is used to obtain different samples, ii) a tree is built on each sample using recursive binary splitting to partition the feature space into different leaves, iii) for a new input \mathbf{x} , the forest produces an output by first computing weights $w_i(\mathbf{x})$ based on the tree partitions as in (8) and then minimizing the weighted loss function given in (6). Note that the usual formulation of point iii) for a regression random forest is the average of the different regression trees, which is in fact equivalent to minimizing the weighted squared error.

We next describe the precise mechanisms i-iii) for GRF. For resampling, GRF uses subsampling rather than bootstrap, which facilitates the theoretical analysis of the model and ensures asymptotic normality for a small subsampling rate. Subsampling means that a smaller data set is produced by selecting randomly s observations out of n (without replacement unlike the bootstrap). The ratio s/n is called the subsampling fraction. In practice, the default subsampling fraction used in the `grf` package is 50%.

The construction of trees in GRF is similar to Breiman’s random forest: recursive binary splitting is used to optimize greedily some criterion and, at each step, the set of possible predictors for the split is reduced by a random selection of m predictors out of p . In GRF, different criteria are designed specifically for different tasks. For quantile regression, the split should be informative with regard to quantiles, meaning the difference of the quantiles in the two resulting nodes should be maximized. [Athey et al. \(2019\)](#) observed that calculating the quantiles for each split is computationally expensive and a slightly

different strategy is used. A categorical recoding of Y into K classes is used based on a sequence of quantiles of order $\tau_1 \leq \dots \leq \tau_{K-1}$: with P denoting the parent node to be split and $\hat{Q}_{Y|\mathbf{X} \in P}(\tau_k)$ the empirical quantile of Y_i 's for which $\mathbf{X}_i \in P$, we define

$$S_i = \sum_{k=1}^K \mathbb{I}(Y_i \leq \hat{Q}_{Y|\mathbf{X} \in P}(\tau_k)).$$

The split of P into two children C_1, C_2 is chosen to maximize the multiclass criterion

$$L(C_1, C_2) = \frac{\sum_{k=1}^K [\sum_{\mathbf{X}_i \in C_1} \mathbb{I}(S_i = k)]^2}{n_{C_1}} + \frac{\sum_{k=1}^K [\sum_{\mathbf{X}_i \in C_2} \mathbb{I}(S_i = k)]^2}{n_{C_2}},$$

with n_{C_l} the number of observations $\mathbf{X}_i \in C_l$, $l = 1, 2$. The default choice in **grf** is $K = 3$ classes with quantiles of orders $\tau_1 = 0.1$, $\tau_2 = 0.5$ and $\tau_3 = 0.9$.

Finally, the output $\hat{Q}_{\mathbf{x}}(\tau)$ of GRF at input \mathbf{x} is computed by minimizing the weighted loss function given in (6) where the weights $w_i(\mathbf{x})$ are computed thanks to the trees as in (8). This produces an dishonest random forest in the terminology of [Athey et al. \(2019\)](#). Honesty is a new and important feature aiming at disentangling the tree construction (splits) and the tree weights (7). For the construction of an honest forest, the subsample \mathcal{D}_b of size s is split into two sets \mathcal{I}_b and \mathcal{J}_b , each of size $s/2$. The tree T_b is constructed on subsample \mathcal{J}_b while the weights are computed on subsample \mathcal{I}_b by

$$w_{i,b}(\mathbf{x}) = \frac{\mathbb{I}\{\mathbf{X}_i \in L_b(\mathbf{x}) \ \& \ i \in \mathcal{I}_b\}}{\sum_{k \in \mathcal{I}_b} \mathbb{I}\{\mathbf{X}_k \in L_b(\mathbf{x})\}}. \quad (19)$$

Here $L_b(\mathbf{x})$ denotes the leaf in T_b that contains \mathbf{x} and we use the convention $0/0 = 0$. This formula for the tree weights is akin to (7) and the forest weights are obtained by averaging as in (8).

Out-of-bag quantile estimates

It has been observed that the quantile $Q_{\mathbf{X}_i}(\tau)$ at an observation point \mathbf{X}_i is not well

estimated. The reason behind this can be traced back to the weights (8): when $\mathbf{x} = \mathbf{X}_i$, the probability weights $(w_k(\mathbf{x}))_{1 \leq k \leq n}$ put too much mass at the i th observation such that the value Y_i has too much leverage on the estimation $\hat{Q}_{\mathbf{X}_i}(\tau)$.

To fix this problem, out-of-bag weights are used. Observation (\mathbf{X}_i, Y_i) is called out-of-bag in the subsample \mathcal{D}_b if $(\mathbf{X}_i, Y_i) \notin \mathcal{D}_b$. Out-of-bag weights are computed using only the sub-forest \mathcal{F}_i consisting of trees T_b for which (\mathbf{X}_i, Y_i) is out of bag, that is

$$\mathcal{F}_i = \{T_b : (\mathbf{X}_i, Y_i) \notin \mathcal{D}_b\}. \quad (20)$$

The resulting weights are denoted by $(w_k^{oob}(\mathbf{X}_i))_{1 \leq k \leq n}$ with $w_i^{oob}(\mathbf{X}_i) = 0$; they are used to compute the out-of-bag quantile estimator $\hat{Q}_{\mathbf{X}_i}^{oob}(\tau)$.

C Appendix: likelihood derivatives

The gradient boosting algorithm for GPD modeling makes use of the first and second order derivatives of the negative log likelihood $\ell_z(\theta)$, $\theta = (\sigma, \gamma)$ and $z > 0$. They are respectively given by

$$\begin{aligned} \frac{\partial \ell_z}{\partial \sigma}(\theta) &= \frac{1}{\sigma} \left(1 - \frac{(1 + \gamma)z}{\sigma + \gamma z} \right), \\ \frac{\partial \ell_z}{\partial \gamma}(\theta) &= -\frac{1}{\gamma^2} \log \left(1 + \gamma \frac{z}{\sigma} \right) + \frac{(1 + 1/\gamma)z}{\sigma + \gamma z}, \end{aligned}$$

and

$$\begin{aligned} \frac{\partial^2 \ell_z}{\partial \sigma^2}(\theta) &= \frac{1}{\sigma(\sigma + \gamma z)} \left(\frac{z}{\sigma} + \frac{z - \sigma}{\sigma + \gamma z} \right), \\ \frac{\partial^2 \ell_z}{\partial \gamma^2}(\theta) &= \frac{2}{\gamma^3} \log \left(\gamma \frac{z}{\sigma} + 1 \right) - \frac{2z}{\gamma^2(\sigma + \gamma z)} - \frac{(1 + 1/\gamma)z^2}{(\sigma + \gamma z)^2}. \end{aligned}$$

D Appendix: additional plots for the application

Figure 11 shows the cross-validated deviance as a function of the number of trees B for two stations for different depth levels. The deviance behaves quite similar for the three choices of depth parameters and we choose $(D^\sigma, D^\gamma) = (2, 1)$ for all stations. Note that here $\lambda_{scale} = 0.025$ for computational purposes. The optimal B parameter is obtained by a single cross validation with λ_{scale} set to the default value 0.01. Given the choice of depth parameter and λ_{scale} , B is chosen to be 347 for Eelde (left panel) and 312 for Schiphol (right panel).

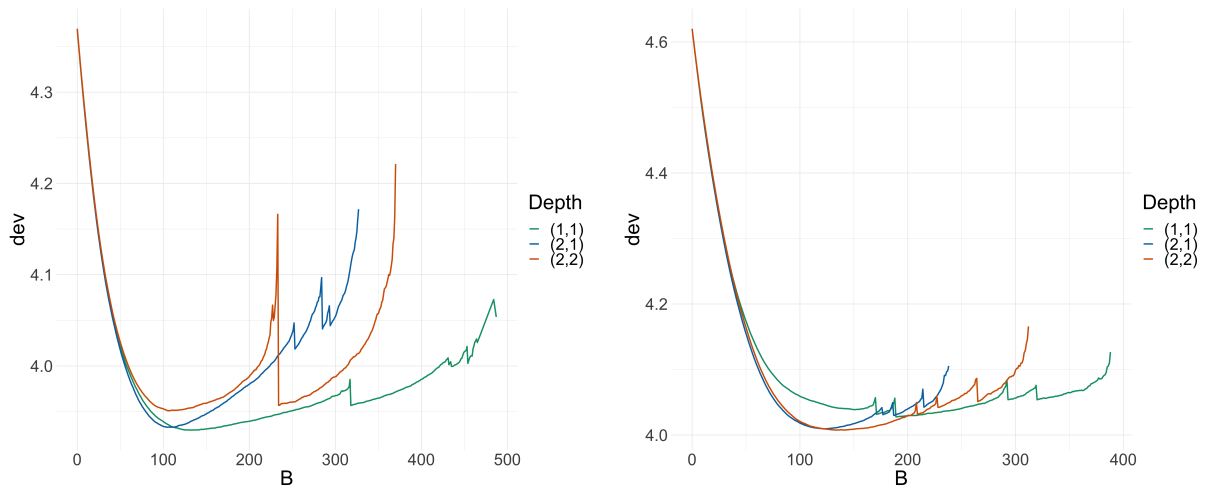


Figure 11: Cross-validation deviance given by (16) against B for the data at stations Eelde (left) and Schiphol (right) in the application in Section 6.

From the assumptions of `gbex` in Section 3, the positive exceedances follow approximately GPD distributions with covariate-dependent parameters. Recall that for station l , $Z_i^{(l)} = (Y_i^{(l)} - \hat{Q}_{\mathbf{X}_i}^{(l)}(0.8))_+$, $1 \leq i \leq n$, and $I^{(l)} = \{i : Z_i^{(l)} > 0\}$ as defined in Algorithm 2.

For $i \in I^{(l)}$, we have that approximately $Z_i^{(l)} \sim \text{GPD}(\hat{\sigma}^{(l)}(\mathbf{X}_i), \hat{\gamma}^{(l)}(\mathbf{X}_i))$, or equivalently,

$$\frac{1}{\hat{\gamma}^{(l)}(\mathbf{X}_i)} \log \left(1 + \frac{\hat{\gamma}^{(l)}(\mathbf{X}_i) Z_i^{(l)}}{\hat{\sigma}^{(l)}(\mathbf{X}_i)} \right) \sim \text{Exp}(1). \quad (21)$$

Based on this, we produce QQ-plots to graphically assess the goodness of fit for the obtained models via **gbex** (left panel) and via the **constant** method (right panel) in Figure 12. It is clear that overall the models estimated by **gbex** fit the data well and are much better than those by the **constant** method.

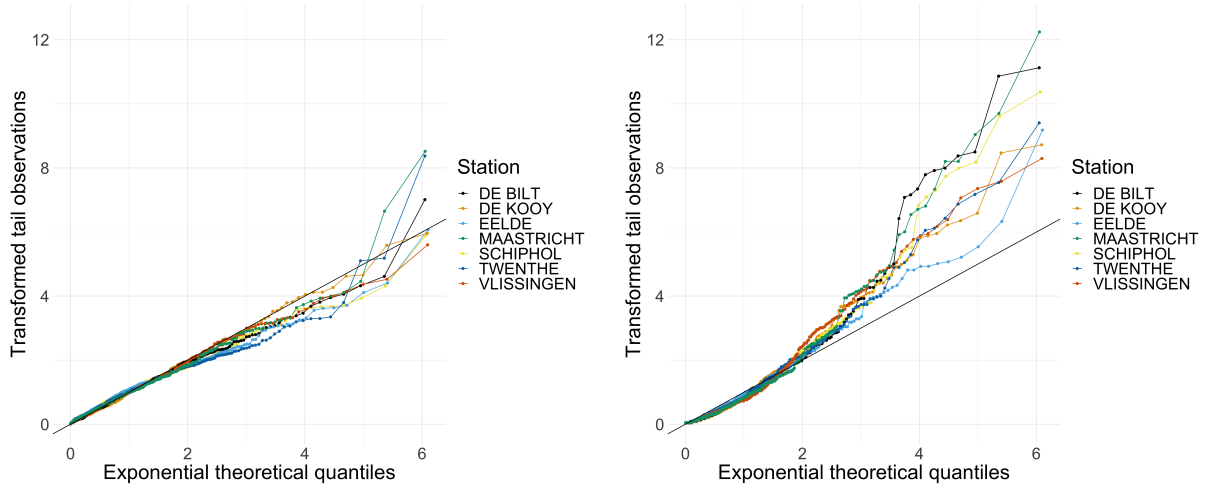


Figure 12: QQ-plots based on (21) for estimated models of seven stations via **gbex** (left panel) and via **constant** method (right panel).